The ZW10 and Rough Deal checkpoint proteins function together in a large, evolutionarily conserved complex targeted to the kinetochore

Frédéric Scaërou[1,*], Daniel A. Starr[2,*], Fabio Piano[2], Ophelia Papoulas[3], Roger E. Karess[1,‡] and Michael L. Goldberg[2,‡]

[1]CNRS, Centre de Génétique Moléculaire, Avenue de la Terrasse, 91198 Gif-sur-Yvette, France
[2]Department of Molecular Biology and Genetics, Biotechnology Building, Cornell University, Ithaca, NY 14853, USA
[3]Department of Biology, Sinsheimer Labs, University of California at Santa Cruz, Santa Cruz, CA 95064, USA
*The first two authors contributed equally to this work
‡Authors for correspondence (e-mail: karess@cgm.cnrs-gif.fr; mlg11@cornell.edu)

Accepted 23 May 2001
Journal of Cell Science 114, 3103-3114 (2001) © The Company of Biologists Ltd

SUMMARY

The *zeste-white 10* (*zw10*) and *rough deal* (*rod*) genes of *Drosophila* both encode kinetochore components, and mutations in either gene greatly increase the missegregation of sister chromatids during mitosis. Here, we present genetic, cytological and biochemical evidence for a close, evolutionarily conserved relationship between the ROD and ZW10 proteins. We show that the phenotypes caused by disruption of either gene's function are similar in *Drosophila* and in *C. elegans.* No additive effects are observed in *zw10; rod* double null mutants. In flies, the two proteins always colocalize and, moreover, require each other for their recruitment to the mitotic apparatus. The human ROD and ZW10 homologs also colocalize on HeLa cell kinetochores or kinetochore microtubules throughout most but not all of mitosis. Finally, we show that in both *Drosophila* and human cells, ROD and ZW10 are in fact physically associated, and in *Drosophila* these proteins are together constituents of a large (700-900 kDa), soluble macromolecular complex.

Key words: Mitosis, Kinetochore, Centromere, Chromosome segregation, Metaphase checkpoint

INTRODUCTION

Faithful transmission of genetic information during cell division is critical to cells and organisms. In humans, for example, mistakes in chromosome segregation during either meiotic division yield aneuploid zygotes, which often spontaneously abort or develop into individuals with abnormalities such as Down's syndrome (Griffin, 1996; Hassold et al., 1996). Mitotic chromosome instability is associated with the progression to cancer in many human tumors (Hartwell and Kastan, 1994), and misregulation of mitosis has recently been correlated with human ageing (Ly et al., 2000).

An evolutionarily conserved surveillance mechanism called the spindle assembly (or metaphase) checkpoint normally prevents the onset of anaphase until all chromosomes are properly attached and aligned on the spindle (reviewed by Amon, 1999; Elledge, 1996; Hardwick, 1998; Nicklas, 1997). In response to an unattached kinetochore, the checkpoint apparatus elaborates an inhibitory signal that delays anaphase onset (reviewed by Nicklas, 1997; Rieder and Salmon, 1998). This inhibitory signal prevents the anaphase promoting complex (APC) from ubiquitinating substrates whose degradation is a prerequisite both for sister chromatid separation and for other aspects of mitotic exit (Morgan, 1999; Zachariae and Nasmyth, 1999). Many of the proteins comprising the spindle checkpoint were first identified in budding yeast by mutations that allowed mitosis to continue when spindles were damaged (Hoyt et al., 1991; Li and Murray, 1991). Homologs of these components function in metazoans, where they have been shown to be transient components of chromosome kinetochores (see below).

Our laboratories have been studying two kinetochore components: Zeste-White 10 (ZW10) and Rough Deal (ROD), originally identified in *Drosophila*, but conserved among multicellular eukaryotes (Karess and Glover, 1989; Scaerou et al., 1999; Starr et al., 1997; Starr et al., 1998; Williams et al., 1992; Williams and Goldberg, 1994; Williams et al., 1996). Null mutations in the *Drosophila* gene encoding either protein provoke similar chromosome segregation defects, including lagging or misdirected chromatids or chromosomes at anaphase, which lead to high levels of aneuploidy in mitotic divisions and in both meiotic divisions in males. Recently, both ROD and ZW10 have been shown to fit the paradigm of true metaphase checkpoint components in *Drosophila* and human cells (Basto et al., 2000; Chan et al., 2000; Savoian et al., 2000). In their absence, cells no longer arrest in response to spindle damage, but rather go on to separate sister chromatids, degrade cyclin B, and exit mitosis, indicating a defect in the checkpoint apparatus. In addition to a function in the spindle checkpoint, it is known that both ROD and ZW10 are needed to target the microtubule motor dynein to the kinetochore (Starr et al., 1998). Impaired chromosome migration to the poles in *zw10* or *rod* mutants is probably due to this absence of dynein at the kinetochore (Savoian et al., 2000).

Immunostaining studies show that ROD and ZW10 display similar dynamic behavior in terms of their intracellular location during the *Drosophila* cell cycle (Scaerou et al., 1999; Williams and Goldberg, 1994). These proteins are found most strongly at the kinetochore during prometaphase. By metaphase, ZW10 and ROD are instead preferentially localized on the kinetochore microtubules (kMTs). At anaphase onset, the proteins disappear from the kMTs and again are found on the kinetochores, at the leading edge of the separating chromosomes. They remain at the kinetochores until they are excluded from the re-forming nuclei during telophase.

Importantly, the association of ZW10 protein with the kinetochore is sensitive to tension across individual chromosomes (Williams et al., 1996). For example, we examined *Drosophila* spermatocytes at meiotic metaphase I that simultaneously contain univalents (chromosomes that remain unpaired during meiosis I) and bivalents (normally paired homologous chromosomes). ZW10 protein levels are much higher on the kinetochore of univalents that do not reach the metaphase plate than on the kinetochores of the bivalents aligned at the metaphase plate. Thus, the localization of ZW10 relative to the kinetochore reflects bipolar tension exerted across individual chromosomes or chromosome pairs.

Many components of the spindle checkpoint similarly localize specifically to the kinetochores of chromosomes that have not acquired a bipolar orientation at the metaphase plate (Chen et al., 1996; Jablonski et al., 1998; Li and Benezra, 1996; Martinez-Exposito et al., 1999; Taylor et al., 1998; Taylor and McKeon, 1997; Waters et al., 1998). Moreover, mutations in genes encoding spindle checkpoint proteins prevent metaphase arrest in response to microtubule poisons, as do mutations in *zw10* or *rod* (Basto et al., 2000; Basu et al., 1999; Chan et al., 2000; Hoyt et al., 1991; Li and Murray, 1991). In spite of these parallels, recent observations suggest that ZW10 and ROD might act independently of the canonical spindle checkpoint. For example, mutations in fly *zw10* or *rod* do not prevent the binding of the checkpoint proteins Bub1 or Bub3 to the kinetochore, while mutations in *bub1* similarly do not block ZW10's association with the kinetochore (Basu et al., 1999; Basu et al., 1998).

Because the ROD and ZW10 proteins behave similarly during mitosis and because mutations in either gene have similar effects, we were prompted to examine the possibility that the two proteins execute their function together. Here, we present genetic, cytological and biochemical evidence for an intimate relationship between ROD and ZW10. We show that disruption of either gene's function causes similar mitotic phenotypes in *Drosophila* neuroblasts and in *C. elegans* embryos. We observe no additive effects in double null mutants in *Drosophila*, suggesting that ROD and ZW10 participate in the same pathway. In flies, the two proteins always colocalize and require each other for their recruitment to the mitotic apparatus. The human ROD and ZW10 proteins usually but not always colocalize in HeLa cells throughout mitosis. Finally, we show that both proteins are constituents of a large, evolutionarily conserved macromolecular complex.

MATERIALS AND METHODS

Fly stocks

The *Drosophila* stocks used in these experiments have been previously described (Williams et al., 1996 (for *zw10*); Karess and Glover, 1989; Scaerou et al., 1999 (for *rough deal*)). Flies were raised on standard medium at 25°C. The mutant alleles employed here ($zw10^{S1}$ and rod^{X5}) are both genetic nulls (Scaerou et al., 1999; Williams et al., 1992).

Identification of ROD homologs

DmROD homologs in other organisms were inferred from tblastn searches of GenBank, which detected human cDNA KIAA0166 (Nagase et al., 1996), GenBank accession number P50748; and *C. elegans* ESTs yk9c3 and yk9c6, accession number AAB00646. ROD ESTs from mouse (AA690110) and rat (BE104266) were also detected. KIAA0166 was obtained from Kazusa DNA Research Institute (Chiba, Japan), and the worm clones from Yuji Kohara (National Institute of Genetics, Mishima, Japan).

Molecular biology techniques

High density colony screening and the cloning of genomic and cDNA fragments were done with standard protocols (Sambrook et al., 1989). DNA was purifed on Qiaprep columns (Qiagen SA, Courtaboeuf, France). The Sequenase kit (Amersham Pharmacia Biotech, Orsay, France) was used for DNA sequencing. Oligonucleotides were synthesized by Eurogentec (Seraing, Belgium), or Isoprim (Toulouse, France).

Antibody production

DmZW10 and HsZW10 antibodies are as described (Williams et al., 1992; Starr et al., 1997). DmROD antibody BE40 is described elsewhere (Scaerou et al., 1999). Anti-HsROD antibody was generated as follows. A 0.7 kb *Hin*dIII fragment of cDNA KIAA0166, encoding amino acids 1738-1985 of the predicted HsROD protein, was ligated to the His6 tag of pET21b (Novagen, Darmstadt, Germany). The protein was expressed in BL21 (DE3) *E. coli* cells after induction by 1 mM IPTG. 600 μg of tagged protein was purified on a Ni affinity column, and sent to Agrobio (Villeny, France) to produce antibody in chickens. The whole IgY fraction was purified by Agrobio from immunized chicken eggs according to (Akita and Nakai, 1993). The antibody was affinity purified by elution from an immunoblot strip (Harlow and Lane, 1982) containing the 30 kDa fusion protein. Affinity purified chicken anti-Rod antibody recognized a high molecular weight protein in HeLa cell extracts, consistent with the size expected for HsROD (250 kDa). Preimmune serum did not detect this band, nor did preimmune serum immunostain any obvious intracellular cell structures (data not shown).

Indirect immunofluorescence of *Drosophila* tissues and human tissue culture cells

Brains and testes were dissected from third instar *Drosophila* larvae and prepared for immunofluorescence as described (Williams and Goldberg, 1994). Testes were dissected either from late third instar or early pupal stage animals, and prepared as described (Williams et al., 1996). Both affinity-purified and crude anti-DmROD sera (Scaerou et al., 1999) were used for immunostaining, and gave identical results. Antibodies were used at the following dilutions: crude rabbit BE40 anti-DmROD, 1/500; crude mouse anti-DmZW10 (Williams et al., 1996), 1/500; Texas Red anti-mouse IgG and FITC anti-rabbit IgG (Jackson ImmunoResearch, West Grove, PA) 1/50; Alexa 594 and 488 anti-mouse and anti-rabbit IgGs (Molecular Probes, Eugene, OR), 1/300. DNA was labeled with DAPI at 0.5 μg/ml.

Unsynchronized HeLa cells were grown in MEM supplemented with L-glutamine (2 mM), penicillin (100 U/ml), streptomycin (100 mg/ml), and 10% FCS (all from Sigma Chemical Co., Saint-Quentin Fallavier, France) at 37°C in 5% CO_2. Cells were plated on 14×14 mm glass coverslips in six-well dishes and grown for 24-48 hours to reach 70-80% confluency.

For triple staining, HeLa cells were rinsed in PHEM (60 mM Pipes, 25 mM Hepes, 10 mM EGTA, 1 mM Mg-acetate, pH 6.9) at 37°C,

treated for 60 seconds with 0.5% Triton X-100 in PHEM to remove excess soluble protein, and fixed for 20 minutes in 3% paraformaldehyde, 0.5% Triton X-100 in PHEM at room temperature. Cells were then washed three times for 7 minutes in PBS, permeabilized for 25 minutes in 0.5% Triton X-100 in PBS, washed twice for 3 minutes in PBS, and incubated for 10 min in 50 mM NH_4Cl. After three 5 minute washes in PBS and two 10 minute washes in PBS/BSA (PBS with 0.1% BSA), the coverslips were incubated with primary antibodies for 1 hour at 37°C, washed three times for 10 minutes with PBS/BSA, incubated with secondary antibodies for 45 minutes at 37°C and washed three times for 10 minutes with PBS. Chromosomes were stained with DAPI (Sigma) at 0.5 μg/ml for 10 minutes. After a rinse with PBS, the coverslips were mounted in mowiol (Hoechst, Frankfurt, Germany) containing 1,4-diazabicyclo-(2,2,2)octane (Sigma) at 100 mg/ml (Langanger et al., 1983).

Primary antibodies for staining HeLa cells were used as follows: affinity-purified anti-HsROD at a dilution of 1/50 in PBS/BSA, affinity-purified anti-HsZW10 at 1:100 (Starr et al., 1997), human CREST serum at 1/100, and monoclonal anti-β-tubulin (Zymed Laboratories, South San Francisco, CA) at 1/20. CREST autoimmune anti-serum (a kind gift from H. Ponstingl, German Cancer Research Center, Heidelberg, Germany) recognizes the centromere components CENP-A, CENP-B and CENP-C (Moroi et al., 1980). All secondary antibodies were made in goat and conjugated to FITC or rhodamine (Jackson ImmunoResearch), or to Cy3 or Cy5 (Sigma).

Microscopy and image analysis

Brains of *Drosophila* third instar larvae were dissected, fixed and stained with aceto-orcein as previously described (Karess and Glover, 1989). Preparations were viewed with a 63× objective using a Nikon Microphot microscope with phase contrast and epifluorescence. Images were collected with a Princeton Instruments cooled CCD camera (Evry, France) using GRAFTEK Fluorograb software (Mirmande, France).

All HeLa cell figures were obtained by three-dimensional wide-field epifluorescence microscopy with a 100× objective on a Leica DM RXA microscope equipped with a Physiks Piezo translocator. Pictures were acquired using Metamorph (Universal Imaging Corporation, West Chester, PA). Z-series of each wavelength were acquired in Z-stream mode using a Princeton Micromax 1300Y5 MHz interline camera. Selective Leica/Chroma filter blocks mounted on the motorized filter turret were used for wavelength selection. Image stacks were deconvoluted using a custom made Metamorph module. Ten to fifteen images of the deconvoluted stacks were used for 3D reconstruction and assembled with Adobe Photoshop 5.0 (Adobe Systems Inc., Mountain View, CA).

C. elegans antisense mRNA injections

C. elegans rod ESTs yk9c3 and yk9c6 were cloned into the *Eco*RI and *Kpn*I sites of pBluescript SK (Stratagene, Amsterdam, The Netherlands). The Ribomax kit (Promega, Madison, Wisconsin) was used to generate in vitro transcribed sense (from the T3 promoter) and antisense (from the T7 promoter) RNA from linearized plasmids. These RNAs were mixed in equal amounts before injection into wild-type (N2) young adults at a final concentration of 300 ng/μl. Water-injected and non-injected worms were negative controls. Individual injected or control worms were plated at 20°C and transferred to new plates daily. Embryonic lethality (failure to hatch) and brood size (numbers of embryos produced) were monitored for 24-48 hours post injection. Embryos from some injected worms were fixed and stained with DAPI as previously described (Etemad-Moghadam et al., 1995) to observe mitotic chromatin.

Protein extraction and immunoblotting

Protein extracts resuspended in loading buffer (CytoSignal, Irvine, CA) and boiled for 5 minute were loaded onto SDS (5-8%)-polyacrylamide gels. Proteins were transferred to nitrocellulose or Immobilon-P membranes (Millipore, Bedford, MA) using a semi-dry electrophoretic blotting device. To facilitate transfer of the large ROD protein, methanol and SDS were omitted from the transfer buffer (25 mM Tris, 192 mM glycine, pH 8.3). Membranes were blocked for 1 hour in TBST (20 mM Tris, 137 mM NaCl, 0.2% Tween, pH 7.6) plus 5% dry milk and incubated overnight at 4°C with one of the following antibodies diluted in TBST+milk: anti-HsZW10 (Starr et al., 1997) at a 1/250 dilution; crude anti-HsROD antisera at 1/1000; anti-DmZW10 (Williams et al., 1992) at 1/2000; or crude anti-DmROD (Scaerou et al., 1999) at 1/1000. After washing in TBST, the blot was incubated with secondary antibody (a 1/5000 dilution of goat anti-rabbit IgG or goat anti-chicken IgY conjugated to horseradish-peroxidase; Jackson ImmunoResearch) at room temperature for 1 hour. Immunodetection was carried out with the ECL kit (Amersham Pharmacia Biotech).

Immunoprecipitations

The protocol from the IMMUNOcatcher kit (CytoSignal) was followed with some minor modifications. 50 μl of 0-16 hour *Drosophila* embryos, 300 dissected larval brains, or S2 *Drosophila* cells from 75 cm^2 flasks were added to 450 μl mild lysis buffer and 50 μl 10× protease inhibitors (CytoSignal), and ground in an eppendorf tube on ice with a pestle. HeLa cells from two nearly confluent 75 cm^2 flasks were collected by trypsinization. The cell pellet was resuspended in 450 μl mild lysis buffer and 50 μl 10× protease inhibitors and homogenized in a 7 ml glass Dounce tissue grinder (Wheaton, Millville, NJ).

After cell lysis during incubation on ice for 30 minutes, insoluble material was removed in a microcentrifuge in a 30 minute spin. The soluble extracts were then pre-cleared for 30 minutes with 50 μl protein A/G resin (CytoSignal) or 50 μl anti-chicken IgY agarose beads (Promega, Madison, WI) and 30 μl of the relevant pre-immune serum. 100 μl of precleared lysate were added to 80 μl of mild lysis buffer and one of the following antibodies: 2 μl of purified anti-*Drosophila* ZW10 antibody, 3 μl of pre-immune serum from the same rabbit, 3 μl of crude anti-*DmROD* antibody, 3 μl of the corresponding pre-immune serum, 3 μl of anti-HsZW10 purified antibody, 3 μl of the same rabbit's pre-immune sera, and 10 μl of chicken anti-HsROD crude IgY, or 10 μl of pre-immune IgY from the same chicken. These solutions were mixed at room temperature for 1 hour. 10 μl protein A/G resin or 50 μl anti-chicken IgY agarose beads were then added for an additional 30 minutes. The beads were collected by 5 second pulses in a microcentrifuge, and then washed five times in mild lysis buffer. Adsorbed proteins were eluted in 40 μl SDS-PAGE loading buffer. 10 μl of the HsZW10 or DmZW10 and 20μl of the HsROD or DmROD immunoprecipitations were subjected to SDS-PAGE. Western blot analysis using anti-ZW10 or anti-ROD antibodies was carried out as described above.

Gel exclusion chromatography of *Drosophila* embryonic extracts

3 mg of soluble *Drosophila* embryo extract was prepared as described (Papoulas et al., 1998) and run over a Superose 6 sizing column (Amersham Pharmacia Biotech). 90 μl aliquots of fractions 13 (the first protein-containing fraction) through 42 (the salt front) were added to 90 μl of 2× SDS loading dye. SDS-PAGE was performed on 20 μl of diluted fractions 15-32 on 5% acrylamide gels, and western blots were probed for DmZW10 or DmROD as above.

Yeast two hybrid assays

To test for direct interactions between HsZW10 and HsROD, we used the yeast two-hybrid system (Bai and Elledge, 1996). The ZW10 prey construct in the vector pACTII has been previously described (Starr et al., 1998), as has the control Hzwint-1 bait construct in the vector pAS2 (Starr et al., 2000). The HsROD open reading frame was divided by PCR amplification into three approximately equal overlapping fragments: HsROD I (residues 1-753), HsROD II (residues 715-1485),

and HsROD III (residues 1455-2210). PCR primers for HsROD I and II included restriction sites for *Bam*H1 and *Eco*R1, while the primers for HsROD III included *Sma*I and *Bgl*II sites. These sections of the HsROD open reading frame were cloned into the polylinker of the pAS2 bait vector downstream of, and in frame with, the GAL4 DNA binding domain. The combinations of bait and prey plasmids shown in Table 2 were co-transformed into the yeast host strain Y190, and β-galactosidase assays of reporter gene expression were performed as described (Bai and Elledge, 1996).

RESULTS

Drosophila ZW10 and ROD function genetically in the same pathway

The similarity in phenotypes caused by null mutations in the *Drosophila zw10* and *rod* genes originally suggested that the two gene products might function together. Animals mutant for either gene usually die during late larval or pupal stages. Although a few mutant adults eclose, these escapers have rough eyes, are sterile, and die within a few days. A high proportion of both *zw10* and *rod* mutant brain cells are aneuploid, with a distribution of abnormal karyotypes suggesting random chromosome missegregation. In both kinds of mutant cells, the spindle looks normal throughout mitosis, but chromosome movements during anaphase are highly disrupted, leading to lagging chromatids, anaphase bridges and aneuploidy. The two sister chromatids often migrate to the same spindle pole, producing daughter cells with unequal chromosome complements. Another intriguing result of *zw10* and *rod* mutations is premature sister chromatid separation (PSCS) (Williams et al., 1992; Scaerou et al., 1999) and cyclin B degradation in the presence of colchicine (Basto et al., 2000). As described above, this phenomenon indicates that the normal spindle checkpoint is bypassed in *zw10* and *rod* mutants.

To test the hypothesis that the *zw10* and *rod* genes function together in the same pathway, we examined larval brains simultaneously mutant for both genes. We found that the two principal aspects of the cytological phenotype, abnormal anaphases and PSCS after colchicine treatment, occur at the same frequency in the *zw10;rod* double mutants as in each mutant alone (Table 1). No additive effect was observed: the range of defects is quantitatively and qualitatively comparable with that for either single mutant. This result reinforces the hypothesis that ZW10 and ROD participate in the same biochemical process influencing chromosome segregation. Moreover, it suggests that neither protein provides an essential function independent of the other.

Table 1. The mitotic phenotype of the *zw10; rod* double mutant is identical to that of either mutant alone

	Untreated brains		Colchicine-treated brains	
Genotype	Abnormal anaphases (%)*	Mitotic index‡	PSCS (%)¶	Mitotic index
Wild-type	2.8 (4/139)	1.02 (636/623)	0.96 (7/670)	2.44 (1584/650)
rod	39.4 (43/109)	0.92 (435/475)	38.2 (142/372)	0.66 (594/900)
zw10	42.3 (33/78)	0.88 (313/355)	35.8 (78/218)	0.71 (170/249)
zw10 rod	41.3 (55/133)	1.07 (762/714)	36.1 (184/509)	0.7 (509/722)

*Abnormal anaphases were scored in untreated 3rd instar larval brains. The numbers in parentheses indicate the number of anaphase figures displaying lagging chromatids, chromatin bridges, and nondisjunction/the total number of anaphases scored.

‡The mitotic index is expressed as the average number of mitotic nuclei (all stages) per optic field. In parentheses is indicated the number of cells in division/number of optic fields scored.

¶Premature sister chromatid separation (PSCS) was scored in 3rd instar larval brains following incubation for 1 hour in colchicine and brief hypotonic shock. The figures in parentheses indicate the number of metaphases in which one or more pairs of sister chromatids are fully separated/the total number of mitotic cells scored.

ROD and ZW10 localization to the mitotic apparatus is identical and mutually dependent in *Drosophila*

The above results suggested that ZW10 and ROD act together. Previous reports had independently described similar dynamic patterns of localization throughout the cell cycle for these two proteins in flies (Scaerou et al., 1999; Williams and Goldberg, 1994). To compare their distributions directly, we simultaneously monitored both proteins in the same cell by double immunofluorescence. We found that during mitosis (Fig. 1a-d), and both male meiotic divisions (not shown), the patterns displayed by both proteins are essentially superimposable. DmZW10 and DmROD are both associated with the kinetochores, then are found irregularly distributed along the kinetochore microtubules (kMTs) in metaphase, and are principally associated with the kinetochores during anaphase. The close correspondence in behavior and distribution of the two proteins is particularly evident when one compares the irregular staining along the kinetochore microtubules during metaphase (Fig. 1b).

Not only are DmZW10 and DmROD found in the same places at the same times, but also each protein requires the other to achieve its localization. We previously showed that the association of DmZW10 with kinetochores or kMTs is abolished in *rod* mutant neuroblasts and spermatocytes (Williams and Goldberg, 1994). Here, we demonstrate that the reverse is also true. DmROD protein fails to localize to kinetochores or kMTs in *zw10* mutant neuroblasts (Fig. 1e,f) or spermatocytes (data not shown). This finding verifies that the two proteins participate in the same pathway, and further implies that ZW10 and ROD exist together in a protein complex.

We next asked whether the distribution of DmROD is different on bi-oriented or mono-oriented chromosomes. DmZW10 has been shown previously to localize along kMTs only if the associated chromosome is attached to both poles of the spindle (i.e. bi-oriented). This is strong evidence that DmZW10 behavior is sensitive to tension exerted by the spindle across the kinetochores (Williams et al., 1996). To determine if the same is true for DmROD, we examined its behavior in meiosis I spermatocytes containing attached-X or attached-4 univalent chromosomes. Such univalents, having no pairing partner, possess only a single kinetochore and must therefore be mono-oriented during meiosis I. We found that in these cells, DmROD staining was consistently confined to the kinetochore region of the univalents, and not distributed along the associated kMTs, whereas the bi-oriented chromosomes showed the prominent kMT staining typical of cells in metaphase but only weak kinetochore staining (Fig. 1g). Thus,

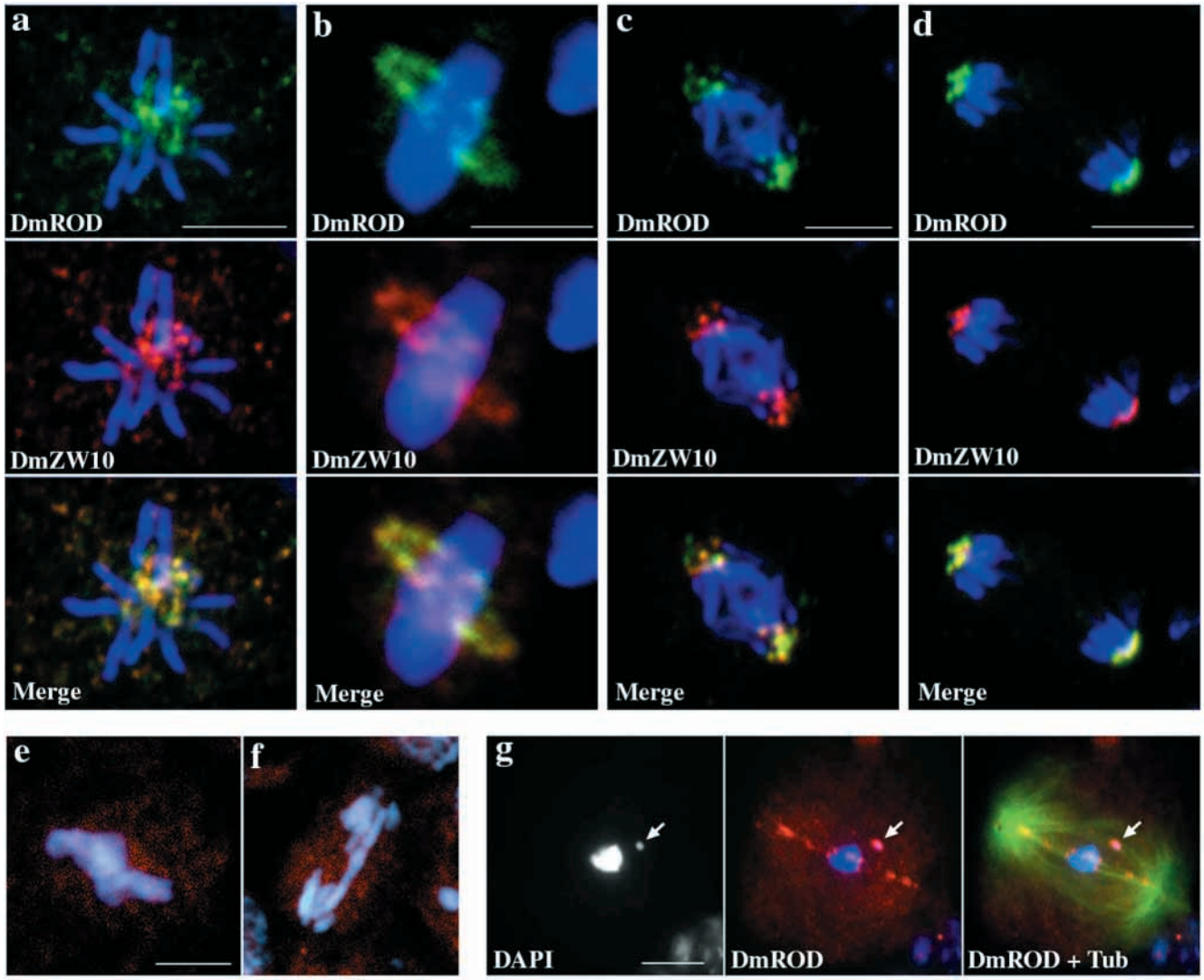

Fig. 1. *Drosophila* ROD and ZW10 protein localization. *Drosophila* ROD and ZW10 proteins colocalize throughout mitosis. (a-d) Wild-type larval brains were fixed and stained to detect ROD (red), ZW10 (green) and DNA (blue). (a) Prometaphase cell; (b) metaphase; (c) early anaphase; (d) late anaphase. The superimposition of ROD and ZW10 signals is shown in the merged images of each set. ROD and ZW10 are found together on prometaphase kinetochores, on the spindle fibers in metaphase, and on kinetochores of the segregating chromatids in anaphase. ROD fails to localize in a *zw10* mutant background (e,f). Larval brains from *zw10* mutants were fixed and stained to detect ROD (red) and DNA (blue). (e) Metaphase *zw10* cell with chromosomes at the equator. (f) Anaphase *zw10* cell. No discrete ROD staining can be seen in either cell. By western blot, ROD is still present in *zw10* mutant brains at normal levels (data not shown). ROD localization is dependent on tension (g). In metaphase I spermatocytes, ROD distribution differs on bivalent (bi-oriented) and on univalent (mono-oriented) chromosomes. (left) DNA; (center) merged image with DNA in blue and ROD in red; (right) same image with tubulin in green. Spindle fibers stain with ROD only on kMTs attached to bi-oriented bivalents. The attached-4 univalent chromosome (arrow) shows no staining of kMTs, but has a prominent ROD signal on the presumptive kinetochore. Bars, 5 μm.

DmROD, like DmZW10, is influenced by bipolar tension exerted across the kinetochore.

Human ROD and ZW10 proteins have a similar distribution during most of mitosis

Proteins closely related to DmZW10 and DmROD exist in many species of multicellular eukaryotes (although neither protein has an obvious homolog in the genome of *S. cerevisiae*). To see if the intracellular localization of ROD proteins is as evolutionarily conserved as their amino acid sequences, we generated antibodies directed against the human ROD (HsROD) protein. By indirect immunofluorescence with this reagent, we could examine the intracellular distribution of HsROD during mitosis in human cells and compare its behavior with that of DmROD.

In early prophase (Fig. 2a) of fixed asynchronous HeLa cells, HsROD is first seen as puncta that co-localize with a subset of the centromeres (as detected by CREST staining) (Moroi et al., 1980; Earnshaw and Rattner, 1991). By prometaphase, anti-HsROD staining was associated with all centromeres in the double dot pattern expected for a kinetochore protein (Fig. 2b). The HsROD label partially overlaps with and extends to the outside of CREST-reactive sites (Fig. 2b, inset), designating HsROD as a component of

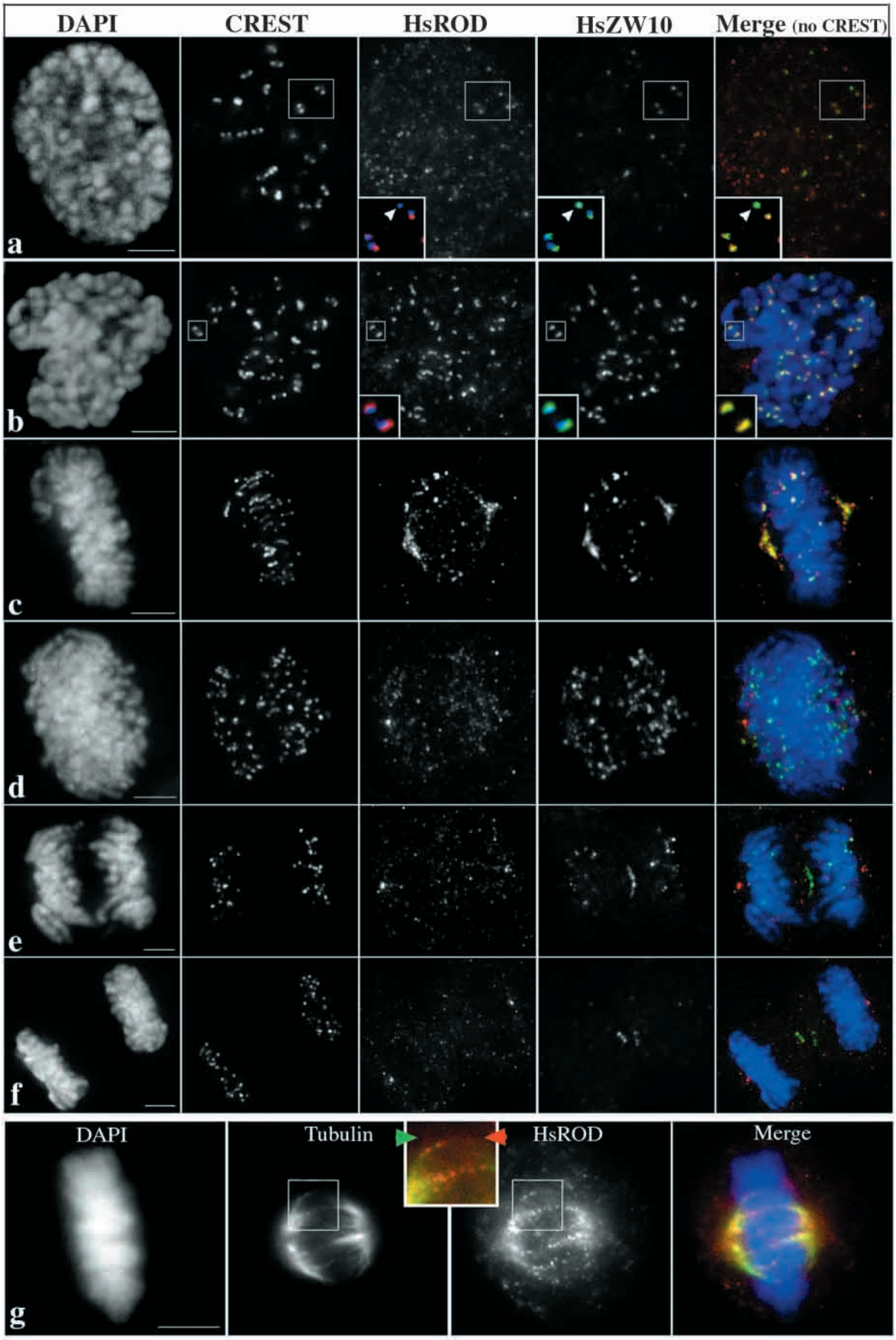
DAPI
CREST
HsROD
HsZW10
Merge (no CREST)
a
b
c
d
e
f
DAPI
Tubulin
HsROD
Merge
g

Fig. 2. Subcellular localization of ROD and ZW10 throughout HeLa cell mitosis. **(**a) Prophase cell. (b) Prometaphase cell. (c,g) Metaphase cells. (d) Early anaphase cell. (e) Late anaphase cell. (f) Telophase cell. The panels show from left to right: DNA, CREST staining, HsROD staining, HsZW10 staining and the superimposition of HsROD and HsZW10 with DNA (b-f) or without DNA (a). For the merged pictures at the right, HsROD was colored in red, HsZW10 in green and DNA in blue. The insets in A and B show higher magnification superimpositions of HsROD (red)/CREST (blue), HsZW10 (green)/CREST (blue) and HsROD (red)/HsZW10 (green). During early prophase (a), HsROD and HsZW10 begin to accumulate near the centromeres of some condensing chromosomes. The HsROD and HsZW10 staining is superimposable and external to the CREST staining. Certain centromeres stain with HsZW10 but not HsROD (arrowhead, inset). During prometaphase (b), both proteins are found in a double dot pattern at every centromere. In metaphase (c,g), when chromosomes are at the spindle equator, both HsROD and HsZW10 decorate kinetochore spindle fibers in an irregular pattern (g), particularly near the poles. By early anaphase (D), HsROD largely disappears from kinetochores, whereas HsZW10 is still detectable on the kinetochores of the segregating chromosomes. As anaphase (d,e) progresses to telophase (f), HsZW10 diminishes at the kinetochore, but gains prominence at the spindle midzone. By contrast, HsROD persists at the spindle poles. By telophase (f), the major HsROD and HsZW10 signals are at the spindle poles and midzone, respectively. All images are projections of 10-15 optical section stacks. Bars, 5 μm.

the kinetochore or of the fibrous corona just distal to the kinetochore (Earnshaw and Rattner, 1991). At metaphase, some HsROD remained near the kinetochores, but most of the protein relocalized to the spindle (Fig. 2c,g), particularly near the spindle poles. As in *Drosophila* cells, the protein appeared to be irregularly distributed along the kinetochore microtubules (Fig. 2g). In very early anaphase (Fig. 2d), discrete HsROD signals were still found at the kinetochores, but at weaker levels than in prometaphase cells. Later in anaphase, HsROD disappeared from the centromeres and accumulated diffusely in the cytoplasm. From late anaphase until the end of telophase, HsROD staining was prominent at the spindle poles (Fig. 2e).

Anti-HsZW10 (Starr et al., 1997) and anti-HsROD antibodies generally, but not always, recognized similar structures in cycling HeLa cells (Fig. 2). We note here a few points of particular interest. (1) In very early prophase cells, some centromeres were decorated by both antibodies, but HsROD was undetectable on some kinetochores that contained HsZW10 (Fig. 2a, insets). (2) By prometaphase (Fig. 2b), both HsROD and HsZW10 invariably decorated all the kinetochores as determined by colocalisation with the CREST serum. (3) When all the chromosomes were aligned at the equator of the cell during metaphase, the brightest staining of both antibodies was found on the spindle near the poles, but some label was also visible on the kinetochores (Fig. 2c). (4) Although HsZW10 and HsROD staining was superimposable, and even maintained the same relative intensity from prometaphase to the onset of anaphase, the two proteins differed in their behavior after anaphase onset. In early anaphase, the HsZW10 staining clearly remained relatively stronger than the HsROD staining on segregating kinetochores (Fig. 2d). Later, the signals diverged further: HsROD signal became relatively prominent at the spindle poles in late anaphase and telophase, while HsZW10 accumulated at the spindle midzone (Fig. 2e,f).

RNA interference of CeROD provokes segregation errors in *C. elegans*

Colocalization of human ZW10 and ROD proteins does not prove that these two proteins execute similar functions in an organism other than *Drosophila*. We thus employed the RNA interference (RNAi) technique to test whether *C. elegans* ROD (CeROD) has an essential role in ensuring reliable chromatid segregation similar to that previously shown for worm ZW10 (Starr et al., 1997). The introduction of double-stranded (ds) RNA into *C. elegans* gonads strongly silences gene expression in a homology-dependent manner (Bosher and Labouesse, 2000). We found that the injection of *Cerod* dsRNA into hermaphrodite female gonads led to a high level of embryonic lethality (greater than 99% among the 1141 embryos collected). No lethality was associated with a control injection.

In each of 20 early cleavage stage embryos examined by fluorescence microscopy, there was at least one, and usually several cells showing clear mitotic abnormalities, particularly chromatin bridges between the two complements of segregating sister chromatids at anaphase (Fig. 3). Similar anaphase chromatin bridges are one of the characteristic features of the *Drosophila rod* phenotype (Karess and Glover, 1989). Embryonic lethality associated with the formation of chromatin bridges is also observed among the progeny of *C. elegans* hermaphrodites injected with antisense *Cezw10* RNA (Starr et al., 1997), indicating that the ZW10 and ROD proteins probably participate in the same evolutionarily conserved process.

ZW10 and ROD proteins physically associate with each other

All the above findings strongly imply that ROD and ZW10 act at the same point in a single pathway to ensure the faithful segregation of chromosomes. This function is evolutionarily conserved in *D. melanogaster*, *C. elegans* and probably humans. Such close cooperation predicts an interaction between ROD and ZW10 proteins at the molecular level. To test whether ROD and ZW10 proteins associate with each other, immunoprecipitations were performed from both

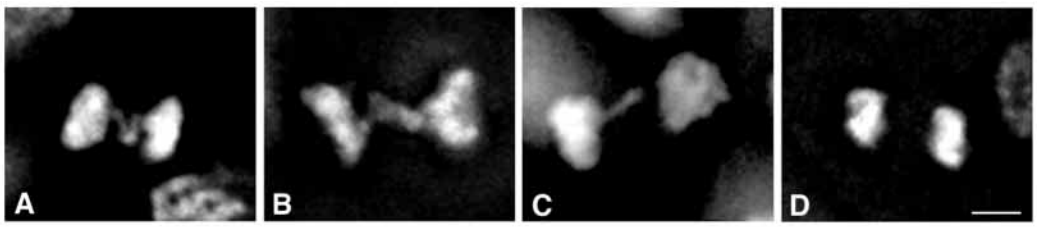

Fig. 3. Chromosome segregation defects in embryos from worms injected with *Cerod* dsRNA. **(**A,B,C) Defective anaphase figures in embryos from worms injected with double stranded *Cerod* RNA. (D) Normal anaphase figure in an embryo obtained from a wild-type hermaphrodite injected with water. Chromatin is stained with DAPI in all panels. Bar, 2 μm.

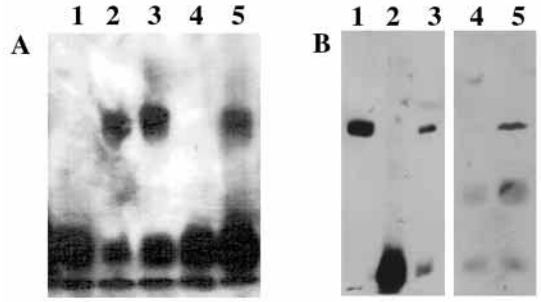

Fig. 4. ZW10 and ROD co-immunoprecipitate from *Drosophila* embryo and HeLa cell extracts. (A) *Drosophila* embryo extracts. Western blot probed with antibodies against DmZW10 shows the presence or absence of DmZW10 in immunoprecipitations from *Drosophila* embryo extracts. Immunoprecipitations used anti-DmZW10 crude (lane 2) or purified sera (lane 3), pre-immune serum from the DmZW10 injected rabbit (lane 1), anti-DmROD crude serum (lane 5), or pre-immune serum from the DmROD injected rabbit (lane 4). (B) HeLa cell extracts. Western blots were probed with antibodies against HsZW10. Lane 1 is crude HeLa cell extract. Other lanes on the blot show immunoprecipitations from the same HeLa cell extract: lane 3, anti-HsZW10 antibody; lane 2, pre-immune serum from the same rabbit; lane 5, anti-HsROD IgY; lane 4, pre-immune IgY from the same chicken. All samples are from the same western blot probed with the same anti-HsZW10 antibody, but the film exposure containing lanes 4 and 5 was for a longer period.

Drosophila embryo and HeLa cell extracts. Fig. 4A shows that ROD and ZW10 co-immunoprecipitate from *Drosophila* embryo extracts. DmZW10 was found in immune complexes using rabbit antibodies directed against DmROD and DmZW10, but not in immune complexes using pre-immune serum from the same rabbits. We also obtained the same result using extracts from larval brains or from *Drosophila* S2 tissue culture cells (data not shown).

We performed analogous immunoprecipitation experiments using extracts from HeLa cells. Fig. 4B shows that human ZW10 and ROD proteins also co-immunoprecipitate. HsZW10 was found in immunoprecipitates with either purified HsZW10 antibody or antibodies against human ROD, but not with either pre-immune serum.

ZW10 and ROD are part of a large soluble complex

The immunoprecipitation experiments above show that ZW10 and ROD are associated in some manner. They could associate with each other as a simple heterodimer, or they might together be part of a larger protein complex. To examine this issue, western blots of a *Drosophila* embryo extract, size-fractionated by gel exclusion chromatography, were probed with antibodies to fly ZW10 and ROD (Fig. 5). DmZW10 and DmROD were both found in fractions corresponding to a size of 700-900 kDa, implying that both antigens are present together in a large stable complex. Velocity sedimentation studies indicate that this complex sediments at approximately 19S (data not shown). A minor peak of ZW10 was found in later fractions that probably represents ZW10 monomers; the ROD signal on the western blot was sufficiently weak that we could not determine if a small proportion of uncomplexed ROD protein was similarly present in the embryo extract.

To examine whether ZW10 and ROD directly contact each other within the context of the 19S complex, we performed a yeast two-hybrid assay (Bai and Elledge, 1996) using either of three overlapping segments of the human ROD protein as bait and a full-length human ZW10 construct as the prey. The results indicated a weak but reproducible interaction between the middle one-third of the HsROD protein (from amino acid residues 715-1485) and HsZW10 (Table 2). However, the signal was clearly less intense than achieved by the positive two-hybrid control between HsZW10 and its previously-identified interactor Hzwint-1 (Starr et al., 2000).

Table 2. HsZW10 and HsROD weakly interact in the yeast two-hybrid assay

Bait construct*	Prey construct‡	β-galactosidase activity¶
HsROD I (1-735)	None	–
HsROD II (715-1485)	None	–
HsROD III (1455-2210)	None	–
HsROD I (1-735)	HsZW10	–
HsROD II (715-1485)	HsZW10	+
HsROD III (1455-2210)	HsZW10	–
None	HsZW10	–
Hzwint-1	HsZW10	++

*Bait constructs were cloned into the pAS2 vector.

‡Prey constructs were cloned into the pACTII vector as described in Materials and Methods (see also Bai and Elledge, 1996).

¶The relative level of β-galactosidase reporter gene activity reproducibly observed in several replicates of Y190 yeast cells transformed with the indicated constructs. The results are consistent with a weak interaction between the middle one-third of HsROD and the HsZW10 protein that is less pronounced than that between HsZW10 and another kinetochore component, Hzwint-1 (Starr et al., 2000).

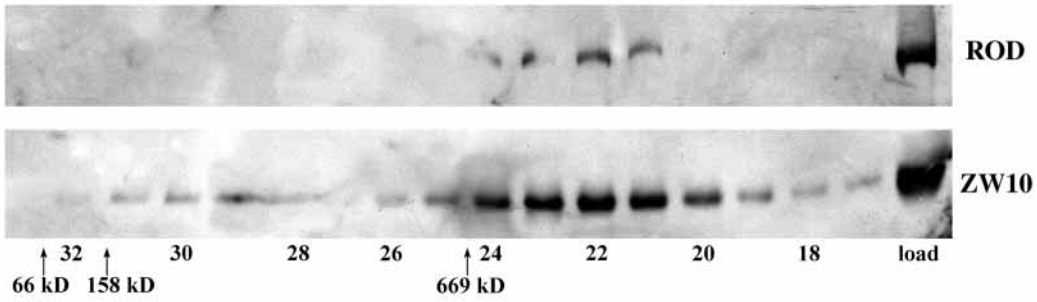

Fig. 5. ZW10 and ROD co-fractionate from a sizing column. (Top) Fractions of a *Drosophila* embryo extract were eluted from a Superose 6 sizing column, transferred to a western blot, and probed with antibodies against DmROD. (Bottom) The same fractions probed with DmZW10 antibodies on a separate blot. Lanes at the far right show DmROD and DmZW10 in the material loaded onto the column. 0.5 ml fractions were collected; the void was at fraction 13, and the salt front in fraction 42. Positions of standards are marked below the blot; 669 kDa (thyroglobulin), 66 kDa (bovine serum albumin), 158 kDa (aldolase).

DISCUSSION

The genetic, immunocytological, and biochemical data presented here show that the ROD and ZW10 proteins are contained within a complex whose activity is required to assure faithful sister chromatid segregation. The amino acid sequences, molecular associations, and at least some of the functions of ROD and ZW10 have been conserved during metazoan evolution. However, because neither protein has a counterpart in *S. cerevisiae*, it is likely that this complex has evolved to accommodate specific needs of metazoan cell division that are not shared in unicellular eukaryotes such as yeast. The three activities that have so far been ascribed to ROD and to ZW10 are: (1) recruiting cytoplasmic dynein to the kinetochore; (2) participating in the poleward movements of chromosomes during mitosis; and (3) maintaining a functional metaphase checkpoint. We discuss below these three functions of ROD and ZW10 in light of the new information presented here.

ROD and ZW10 function in the same pathway within the same complex

ZW10 and ROD share many important genetic and cytological properties. Null mutations in the *Drosophila* genes encoding either protein cause identical phenotypic syndromes (Williams et al., 1992; Karess and Glover, 1989), while depletion of either protein by RNAi in C. *elegans* provokes the same chromosome segregation defects (Starr et al., 1997; Fig. 3). Significantly, the mitotic phenotype of the double *zw10; rod* mutant in *Drosophila* is indistinguishable from that of either mutant alone (Table 1). The two proteins thus appear to act together in the same pathway, and neither protein seems to supply an essential activity independently of the other. The almost identical behavior of the two proteins during mitosis in both *Drosophila* and human cells supports this idea. DmROD and DmZW10 always colocalize on the mitotic apparatus, and both appear to move from the kinetochores to the kMTs in response to tension exerted across the bi-oriented chromosome by the spindle (Williams et al., 1996; Fig. 1). The mutual dependence of the two proteins for their localization to the mitotic apparatus (Williams and Goldberg, 1994; Fig. 1e,f) further emphasizes that neither protein can act independently of the other.

These results suggested that the two proteins might associate with each other within the same macromolecular complex. This prediction was verified by the experiments shown in Figs 4, 5, which demonstrate that ZW10 and ROD can be co-immunoprecipitated from both fly and human cell extracts, and that the two *Drosophila* proteins co-elute from gel filtration columns as a complex of approximately 700-900 kDa. Our finding that HsROD and HsZW10 co-immunoprecipitate has been independently verified in a report that appeared while this article was being prepared for publication (Chan et al., 2000).

We tested for direct interactions between HsROD and HsZW10 using the yeast two-hybrid system previously described (Bai and Elledge, 1996). We observed a relatively weak two-hybrid interaction between HsZW10 and the middle one-third of HsROD (Table 2), suggesting that these two proteins do in fact touch each other within the complex. However, the low level of the signal does not rule out that a third protein might mediate much of the interaction between ROD and ZW10. Since DmROD (240 kDa) and DmZW10 (85 kDa) together account for just under half of the estimated mass, the complex either contains additional components or multiple copies of ZW10 and/or ROD. Further biochemical characterization of the complex will be required to identify other presumptive constituents.

ZW10 and ROD are probably not always associated

Although ROD and ZW10 are sometimes in the same macromolecular complex, the two proteins do not necessarily fulfill identical roles nor do they always have to be associated. For example, in Fig. 5, it appears that *Drosophila* embryo extracts contain some ZW10 protein that elutes from sizing columns at the position expected for uncomplexed monomers. Additional support for this possibility comes from the immunostaining studies in HeLa cells. In prophase (Fig. 2a), some kinetochores apparently contained HsZW10 but not HsROD. HsZW10 might thus be able to assemble transiently onto kinetochores without HsROD, even if the two proteins are mutually required for stable localization to the mitotic apparatus (Fig. 1e,f; Williams and Goldberg, 1994).

The behavior of HsROD and HsZW10 diverges even more following anaphase onset. HsROD leaves the kinetochores before HsZW10 during anaphase. Later on, in telophase, HsROD is observed at the spindle poles, while HsZW10 is found in the spindle midzone. The significance of this apparent separation of HsROD and HsZW10 late in mitosis is unclear. It may simply reflect inactivation and dissociation of the complex, since the total amount of HsROD and HsZW10 associated with mitotic structures decreases significantly after anaphase onset. However, some components of the checkpoint apparatus (Bub2 and Mps1 in *S. cerevisiae*) are found at the spindle poles, where they could potentially interact with ROD (Fraschini et al., 1999; Weiss and Winey, 1996). In addition, cytokinesis sometimes fails in *Drosophila zw10* mutant spermatocytes (Williams et al., 1996), a phenotype often associated with structural defects in the late anaphase spindle midzone (Giansanti et al., 1998).

Although immunofluorescence experiments in *D. melanogaster* show no divergence between ROD and ZW10, we have seen ROD at the spindle poles of *D. simulans* cells by immunostaining with anti-DmROD (data not shown). In addition, visualization of DmROD-GFP *in vivo* suggests that DmROD protein indeed reaches the poles (R. Basto and R.K., unpublished). Thus it remains possible (but far from proven) that the divergent behavior of ZW10 and ROD in human cells is evolutionarily conserved.

Recently, Chan et al. described the localization of HsROD during mitosis in a way that exactly mirrors our description of HsROD behavior in Fig. 2, but with a single exception of possible importance (Chan et al., 2000). They found that in early prophase, some kinetochores stained positive for HsROD but not yet HsZW10. In our Fig. 2a, we show precisely the opposite: some kinetochores at this early stage appear to contain only HsZW10, and not HsROD. The anti-HsZW10 used in both studies was the same. The anti-HsROD, by contrast, was produced against different ends of the protein: the N-terminal region in the case of Chan et al., and a domain near the C-terminus in the present study. The conflict between these results could be explained if various parts of the ROD protein are differentially accessible to antibody staining at the

kinetochore early in mitosis. Any such differences in accessibility would have to be very transient, since both studies found that by nuclear envelope breakdown, all kinetochores label brightly with either anti-ROD probe.

How does the 19S complex participate in kinetochore assembly?

In the absence of either ROD or ZW10, the 19S complex cannot bind kinetochores or recruit dynein, and the spindle checkpoint is no longer functional. The failure of ZW10 to localize to the kinetochore in *rod* mutants, and the failure of ROD to associate with the kinetochore in *zw10* mutants, suggest either that the complex requires all of its components for its stability, or that ZW10 and ROD proteins have a special role among these components either for initial kinetochore targeting or for subsequent maintenance of the complex at the kinetochore.

Several questions concerning the recruitment of the 19S complex to the kinetochore remain unanswered. First, we do not know whether the complex is pre-assembled in the cytoplasm before it associates with kinetochores, or instead whether it is first assembled only at the kinetochore. The reason for this uncertainty is that we prepared our extracts of *Drosophila* embryos and HeLa cells with non-ionic detergents, which may have stripped the complex off of kinetochores and made it soluble. At least in HeLa cells, current data points to assembly at the kinetochore, because some of the early prophase kinetochores shown in Fig. 2a are stained with HsZW10 but not HsROD. Owing to the discrepancy described above between our results and those of Chan et al., we do not regard this situation as conclusively settled.

A second outstanding issue concerns when the 19S complex associates with the kinetochore during the cell cycle: the timing appears to be different in *Drosophila* cells and in human tissue culture cells. Fig. 2 shows that in HeLa cells, HsROD and HsZW10 begin to accumulate on kinetochores by early prophase, clearly prior to nuclear envelope breakdown (NEB). By contrast, the earliest labeling of kinetochores by anti-ROD or anti-ZW10 in *Drosophila* is after NEB, as prophase cells do not show any discrete nuclear localization of ROD or ZW10. We have recently confirmed this latter point by monitoring a GFP-ROD fusion protein in real time in *Drosophila* embryos (R. Basto and R.K., unpublished). The difference between *Drosophila* and human cells is surprising given several studies indicating that human kinetochores are assembled in a reproducible series of steps (Chan et al., 1998; Jablonski et al., 1998). It is possible that the program of kinetochore assembly in *Drosophila* is merely delayed relative to that in humans, but the timing difference may be more significant. The resolution of this issue will require more extensive studies with a panel of antibody reagents directed against proteins at fly kinetochores.

Finally, we do not know what molecules at the kinetochore are required for the targeting of the 19S complex itself. One candidate to recruit the complex to the kinetochore, at least in human cells, is HZwint-1, a kinetochore component we first identified as a strong yeast two-hybrid interactor with HsZW10 (Starr et al., 2000). HZwint-1 associates with kinetochores prior to HsZW10 or HsROD, consistent with a role in targeting the complex to the kinetochore, but no direct evidence to establish this putative activity of HZwint-1 is currently available. Although *Drosophila* has no obvious homolog of HZwint-1, flies could nonetheless have a protein that preserves important elements of its coiled-coil structure.

The ROD/ZW10 complex has multiple functions

Information to date suggests that the 19S complex fulfills at least three functions. One of these functions is to target the microtubule motor cytoplasmic dynein to the kinetochore, probably through a direct interaction of ZW10 with the p50 subunit of dynactin complex (Starr et al., 1998). The involvement of ZW10 and ROD with a known minus-end directed motor could help to explain the apparent movement of these proteins from the kinetochore to kMTs during metaphase. One can imagine further that dynein mediates the response of the complex to spindle tension (Fig. 1g). Finally, the role of ZW10 and ROD in recruiting dynein to the kinetochore can explain a second, recently-described function of these proteins in determining the rate of chromosome movement to the spindle poles. In *zw10* or *rod* mutant spermatocytes, poleward migration of the chromosomes is severely attenuated (Savoian et al., 2000). We note that the roles of the 19S complex in targeting dynein to the kinetochore and thus in chromosome behavior must be metazoan-specific, consistent with the absence of *zw10* or *rod* genes from the *S. cerevisiae* genome. Dynein is excluded from *S. cerevisiae* nuclei (Cottingham et al., 1999; Yeh et al., 1995), and the nuclear envelope does not break down during mitosis in yeast. We thus speculate that dynein's function at the metazoan kinetochore must be supplied by other motor proteins at the yeast kinetochore.

The 19S complex has a third function: it acts in the metaphase checkpoint. It has been clear for several years that sister chromatids separate precociously in *zw10* or *rod* mutant cells treated with colchicine (Gatti and Baker, 1989; Scaerou et al., 1999; Williams et al., 1992). This is not the case in wild-type cells, where the metaphase checkpoint blocks or delays anaphase entry if the spindle is disrupted. Recent evidence (Basto et al., 2000; Chan et al., 2000; Savoian et al., 2000) shows that *zw10* or *rod* mutant cells show no delay in anaphase onset when the spindle is damaged, but in fact exit mitosis and meiosis, as is the case for cells with mutations in genes encoding classical checkpoint components such as the BUB or MAD proteins (Basu et al., 1999; Hoyt et al., 1991; Li and Murray, 1991).

The recruitment of ROD/ZW10 to kinetochores in *Drosophila* does not require the checkpoint proteins BUB1 and BUB3, nor does the kinetochore association of BUB1 or BUB3 require ROD or ZW10 (Basu et al., 1998; Basu et al., 1999; data not shown). Thus, at least at the level of kinetochore targeting, the 19S complex is independent of the classical checkpoint molecules. These results suggest that the checkpoint in metazoan cells has an added layer of complexity, mediated in part by the 19S complex, which is not found in yeast. Mitosis in metazoan cells has important differences from yeast mitosis that might require a more elaborate checkpoint. For example, yeast chromosomes do not congress to a true metaphase plate (Straight et al., 1997). Furthermore, in contrast to metazoans, yeast sister kinetochores separate and are drawn to the poles before the chromatid arms separate and anaphase begins (Goshima and Yanagida, 2000).

In contrast with the reduction of poleward chromosome

movement in *zw10* or *rod* mutants, it is unlikely that the defective checkpoint function in mutant cells is similarly an indirect consequence of the absence of dynein from the kinetochore. Lack of dynein would be expected to activate the checkpoint mechanism by lowering microtubule density at the kinetochore or disrupting tension across chromosomes. In fact, compromising dynein activity at the kinetochores of mammalian cells has been shown to activate the checkpoint, causing cells to arrest in a prometaphase-like state (Echeverri et al., 1996; Nicole et al., 2000). Similarly, cells depleted of CENP-E, another kinetochore-based microtubule motor, can also arrest in mitosis (Schaar et al., 1997). We thus believe that the activities of the 19S complex in recruitment of dynein and in the spindle checkpoint may be distinct. The identification of components in addition to ZW10 and ROD may soon resolve how the 19S complex can simultaneously accomplish its several tasks.

Many thanks to J. De Mey, J. Dompierre, F. Coquelle and J. B. Sibarita (Institut Curie) for their advice and assistance with immunostaining and image processing of the cells in Fig. 2. We thank A. Glatigny and Z. Li for their technical assistance, and R. Basto and B. Williams for helpful discussions and critical reading of the manuscript. F.S. was supported by Le Ministère Nationale de l'Enseignement Supérieur et de la Recherche and the Philippe Foundation. D.S. was supported by NIH training grant GM07617 to the Field of Genetics and Development at Cornell University. This work was supported by grants from the Centre National de la Recherche Scientifique (CNRS) France, and the Association Pour la Recherche sur le Cancer to R. K, and by NIH (USA) grant GM48430 to M.L.G. The work was carried out partly at the Centre de Génétique Moléculaire du CNRS (UPR 2420), and partly at the Cornell University Dept. of Molecular Biology and Genetics.

REFERENCES

Akita, E. M. and Nakai, S. (1993). Production and purification of Fab' fragments from chicken egg yolk immunoglobulin Y (IgY). *J. Immunol. Methods* **162**, 155-164.

Amon, A. (1999). The spindle checkpoint. *Curr. Opin. Genet. Dev.* **9**, 69-75.

Bai, C. and Elledge, S. J. (1996). Gene identification using the yeast two-hybrid system. *Methods Enzymol.* **273**, 331-347.

Basto, R., Gomes, R. and Karess, R. E. (2000). Rough Deal and ZW10 are required for the metaphase checkpoint in *Drosophila*. *Nat. Cell Biol.* **2**, 939-943.

Basu, J., Logarinho, E., Herrmann, S., Bousbaa, H., Li, Z., Chan, G. K., Yen, T. J., Sunkel, C. E. and Goldberg, M. L. (1998). Localization of the *Drosophila* checkpoint control protein Bub3 to the kinetochore requires Bub1 but not ZW10 or Rod. *Chromosoma* **107**, 376-385.

Basu, J., Bousbaa, H., Logarinho, E., Li, Z., Williams, B. C., Lopes, C., Sunkel, C. E. and Goldberg, M. L. (1999). Mutations in the essential spindle checkpoint gene *bub1* cause chromosome missegregation and fail to block apoptosis in *Drosophila*. *J. Cell Biol.* **146**, 13-28.

Bosher, J. M. and Labouesse, M. (2000). RNA interference: genetic wand and genetic watchdog. *Nat. Cell Biol.* **2**, E31-E36.

Chan, G. K., Schaar, B. T. and Yen, T. J. (1998). Characterization of the kinetochore binding domain of CENP-E reveals interactions with the kinetochore proteins CENP-F and hBUBR1. *J. Cell Biol.* **143**, 49-63.

Chan, G. K. T., Jablonski, S. A., Starr, D. A., Goldberg, M. L. and Yen, T. J. (2000). Human ZW10 and Rod kinetochore proteins are novel components of the mitotic checkpoint. *Nat. Cell Biol.* **2**, 944-947.

Chen, R. H., Waters, J. C., Salmon, E. D. and Murray, A. W. (1996). Association of spindle assembly checkpoint component XMAD2 with unattached kinetochores. *Science* **274**, 242-246.

Cottingham, F. R., Gheber, L., Miller, D. L. and Hoyt, M. A. (1999). Novel roles for *Saccharomyces cerevisiae* mitotic spindle motors. *J. Cell Biol.* **147**, 335-350.

Earnshaw, W. C. and Rattner, J. B. (1991). The use of autoantibodies in the study of nuclear and chromosomal organization. *Methods Cell Biol.* **35**, 135-175.

Echeverri, C. J., Paschal, B. M., Vaughan, K. T. and Vallee, R. B. (1996). Molecular characterization of the 50-kDa subunit of dynactin reveals function for the complex in chromosome alignment and spindle organization during mitosis. *J. Cell Biol.* **132**, 617-633.

Elledge, S. J. (1996). Cell cycle checkpoints: preventing an identity crisis. *Science* **274**, 1664-1672.

Etemad-Moghadam, B., Guo, S. and Kemphues, K. J. (1995). Asymmetrically distributed PAR-3 protein contributes to cell polarity and spindle alignment in early *C. elegans* embryos. *Cell* **83**, 743-752.

Fraschini, R., Formenti, E., Lucchini, G. and Piatti, S. (1999). Budding yeast Bub2 is localized at spindle pole bodies and activates the mitotic checkpoint via a different pathway from Mad2. *J. Cell Biol.* **145**, 979-991.

Gatti, M. and Baker, B. S. (1989). Genes controlling essential cell-cycle functions in *Drosophila melanogaster*. *Genes Dev.* **3**, 438-453.

Giansanti, M. G., Bonaccorsi, S., Williams, B., Williams, E. V., Santolamazza, C., Goldberg, M. L. and Gatti, M. (1998). Cooperative interactions between the central spindle and the contractile ring during *Drosophila* cytokinesis. *Genes Dev.* **12**, 396-410.

Goshima, G. and Yanagida, M. (2000). Establishing biorientation occurs with precocious separation of the sister kinetochores, but not the arms, in the early spindle of budding yeast. *Cell* **100**, 619-633.

Griffin, D. K. (1996). The incidence, origin, and etiology of aneuploidy. *Int. Rev. Cytol.* **167**, 263-296.

Hardwick, K. G. (1998). The spindle checkpoint. *Trends Genet.* **14**, 1-4.

Harlow, E. and Lane, D. (1982) *Antibodies.* New York: Cold Spring Harbor Laboratory Press.

Hartwell, L. H. and Kastan, M. B. (1994). Cell cycle control and cancer. *Science* **266**, 1821-1828.

Hassold, T., Abruzzo, M., Adkins, K., Griffin, D., Merrill, M., Millie, E., Saker, D., Shen, J. and Zaragoza, M. (1996). Human aneuploidy: incidence, origin, and etiology. *Environ. Mol. Mutagen.* **28**, 167-175.

Hoyt, M. A., Totis, L. and Roberts, B. T. (1991). *S. cerevisiae* genes required for cell cycle arrest in response to loss of microtubule function. *Cell* **66**, 507-517.

Jablonski, S. A., Chan, G. K., Cooke, C. A., Earnshaw, W. C. and Yen, T. J. (1998). The hBUB1 and hBUBR1 kinases sequentially assemble onto kinetochores during prophase with hBUBR1 concentrating at the kinetochore plates in mitosis. *Chromosoma* **107**, 386-396.

Karess, R. E. and Glover, D. M. (1989). *rough deal*: a gene required for proper mitotic segregation in *Drosophila*. *J. Cell Biol.* **109**, 2951-2961.

Langanger, G., De Mey, J. and Adam, H. (1983). 1,4-Diazobicyclo-(2,2,2)-octane (DABCO) retards the fading of immunofluorescence preparations. *Mikroskopie* **40**, 237-241.

Li, R. and Murray, A. W. (1991). Feedback control of mitosis in budding yeast. *Cell* **66**, 519-531.

Li, Y. and Benezra, R. (1996). Identification of a human mitotic checkpoint gene: hsMAD2. *Science* **274**, 246-248.

Ly, D. W., Lockhart, D. J., Lerner, R. A. and Schultz, P. G. (2000). Mitotic misregulation and human aging. *Science* **287**, 2486-2492.

Martinez-Exposito, M. J., Kaplan, K. B., Copeland, J. and Sorger, P. K. (1999). Retention of the BUB3 checkpoint protein on lagging chromosomes. *Proc. Natl. Acad. Sci. USA* **96**, 8493-8498.

Morgan, D. O. (1999). Regulation of the APC and the exit from mitosis. *Nat. Cell Biol.* **1**, E47-E53.

Moroi, Y., Peebles, C., Fritzler, M. J., Steigerwald, J. and Tan, E. M. (1980). Autoantibody to centromere (kinetochore) in scleroderma sera. *Proc. Natl. Acad. Sci. USA* **77**, 1627-1631.

Nagase, T., Seki, N., Ishikawa, K., Tanaka, A. and Nomura, N. (1996). Prediction of the coding sequences of unidentified human genes. V. The coding sequences of 40 new genes (KIAA0161-KIAA0200) deduced by analysis of cDNA clones from human cell line KG-1. *DNA Res.* **3**, 43-53.

Nicklas, R. B. (1997). How cells get the right chromosomes. *Science* **275**, 632-637.

Nicole, E., Faulkner, N. E., Dujardin, D. L., Tai, C.-Y., Vaughan, K. T., O'Connell, C. B., Wang, Y.-L. and Vallee, R. B. (2000). A role for the lissencephaly gene LIS1 in mitosis and cytoplasmic dynein function. *Nat. Cell Biol.* **2**, 784-791.

Papoulas, O., Beek, S. J., Moseley, S. L., McCallum, C. M., Sarte, M., Shearn, A. and Tamkun, J. W. (1998). The *Drosophila* trithorax group proteins BRM, ASH1 and ASH2 are subunits of distinct protein complexes. *Development* **125**, 3955-3966.

Rieder, C. L. and Salmon, E. D. (1998). The vertebrate cell kinetochore and its roles during mitosis. *Trends Cell Biol.* **8**, 310-318.

Sambrook, J., Fritsch, E. and Maniatis, T. (1989). Molecular Cloning: A Laboratory Manual. New York: Cold Spring Harbor Laboratory Press.

Savoian, M. S., Goldberg, M. L. and Rieder C. L. (2000). The rate of poleward chromosome movement is attentuated in *Drosophila zw10* and *rod* mutants. *Nat. Cell Biol.* 2, 948-952.

Scaerou, F., Aguilera, I., Saunders, R., Kane, N., Blottiere, L. and Karess, R. (1999). The rough deal protein is a new kinetochore component required for accurate chromosome segregation in *Drosophila. J. Cell Sci.* **112**, 3757-3768.

Schaar, B. T., Chan, G. K., Maddox, P., Salmon, E. D. and Yen, T. J. (1997). CENP-E function at kinetochores is essential for chromosome alignment. *J. Cell Biol.* **139**, 1373-1382.

Starr, D. A., Williams, B. C., Li, Z., Etemad-Moghadam, B., Dawe, R. K. and Goldberg, M. L. (1997). Conservation of the centromere/kinetochore protein ZW10. *J. Cell Biol.* **138**, 1289-1301.

Starr, D. A., Williams, B. C., Hays, T. S. and Goldberg, M. L. (1998). ZW10 helps recruit dynactin and dynein to the kinetochore. *J. Cell Biol* **142**, 763-774.

Starr, D. A., Saffery, R., Li, Z., Simpson, A. E., Choo, K. H., Yen, T. J. and Goldberg, M. L. (2000). HZwint-1, a novel human kinetochore component that interacts with HZW10. *J. Cell Sci.* **113**, 1939-1950.

Straight, A. F., Marshall, W. F., Sedat, J. W. and Murray, A. W. (1997). Mitosis in living budding yeast: anaphase A but no metaphase plate. *Science* **277**, 574-578.

Taylor, S. S. and McKeon, F. (1997). Kinetochore localization of murine Bub1 is required for normal mitotic timing and checkpoint response to spindle damage. *Cell* **89**, 727-735.

Taylor, S. S., Ha, E. and McKeon, F. (1998). The human homologue of Bub3 is required for kinetochore localization of Bub1 and a Mad3/Bub1-related protein kinase. *J. Cell Biol.* **142**, 1-11.

Waters, J. C., Chen, R. H., Murray, A. W. and Salmon, E. D. (1998). Localization of Mad2 to kinetochores depends on microtubule attachment, not tension. *J. Cell Biol.* **141**, 1181-1191.

Weiss, E. and Winey, M. (1996). The *Saccharomyces cerevisiae* spindle pole body duplication gene MPS1 is part of a mitotic checkpoint. *J. Cell Biol.* **132**, 111-123.

Williams, B. C., Karr, T. L., Montgomery, J. M. and Goldberg, M. L. (1992). The *Drosophila l(1)zw10* gene product, required for accurate mitotic chromosome segregation, is redistributed at anaphase onset. *J. Cell Biol.* **118**, 759-773.

Williams, B. C. and Goldberg, M. L. (1994). Determinants of *Drosophila* ZW10 protein localization and function. *J. Cell Sci.* **107**, 785-798.

Williams, B. C., Gatti, M. and Goldberg, M. L. (1996). Bipolar spindle attachments affect redistributions of ZW10, a *Drosophila* centromere/kinetochore component required for accurate chromosome segregation. *J. Cell Biol.* **134**, 1127-1140.

Yeh, E., Skibbens, R. V., Cheng, J. W., Salmon, E. D. and Bloom, K. (1995). Spindle dynamics and cell cycle regulation of dynein in the budding yeast, *Saccharomyces cerevisiae. J. Cell Biol.* **130**, 687-700.

Zachariae, W. and Nasmyth, K. (1999). Whose end is destruction: cell division and the anaphase-promoting complex. *Genes Dev.* **13**, 2039-2058.